Inorganic Chemistry

Article

pubs.acs.org/IC

Eu(III) and Tb(III) Complexes with the Nonsteroidal Anti-Inflammatory Drug Carprofen: Synthesis, Crystal Structure, and Photophysical Properties

Xianju Zhou,* Xiaoqi Zhao, Yongjie Wang, Bing Wu, Jun Shen, Li Li, and Qingxu Li

School of Science, Chongqing University of Posts and Telecommunications, 2# Road Chongwen, Chongqing 400065, P. R. China

Supporting Information

ABSTRACT: Two new lanthanide complexes with general formula $[Ln_2(carprofen)_6(DMF)_2]$ (Ln = Eu (**1**), Tb (**2**), DMF = *N*,*N*-dimethylformamide, carprofen = 6-chloro-α-methylcarbazole-2-acetic acid) have been synthesized by a hydrothermal method. Complex **1** was characterized by single-crystal X-ray diffraction (XRD), and it was found to crystallize in the monoclinic space group *C*2/*c*. The coordination of the ligand to the lanthanide ion has been investigated by Fourier-transform infrared (FTIR) spectra and ultraviolet−visible (UV−vis) absorption spectra. Complex **1** emits red light, but the antenna effect of the ligand is not effective, whereas complex **2** presents intense green emission with effective energy transfer from the ligand. The different performance of the two complexes is related to the energy matching between the excited states of the lanthanide ion and the triplet state of the ligand. The intramolecular energy transfer mechanisms are also discussed.

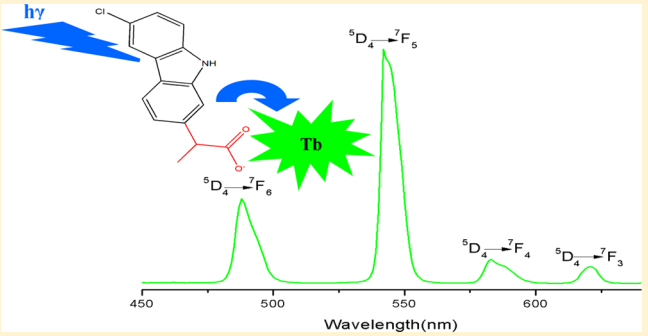

1. INTRODUCTION

Due to their unique photophysical properties, luminescent lanthanide complexes have considerable important applications in a wide range of optical applications, including tunable lasers, plastic optical fiber amplifiers (POFA), multicolor displays, and organic light-emitting diodes (OLEDs).[1−5] In particular, the potential applications in biomedical analyses, cell and tissue imaging, medical diagnosis, and protein labeling have recently aroused more attention.[1,6−12] Luminescent Tb^{3+} and Eu^{3+} complexes are used in homogeneous time-resolved fluorescence (HTRF) technology owing to their long lifetimes, and Eu^{3+} complexes acting as agents have been marketed.[8] Because of the parity-forbidden 4f−4f transitions, trivalent lanthanide cations possess low molar extinction coefficients ($\varepsilon < 1\ M^{-1}\ cm^{-1}$),[11,13] making the direct lanthanide excitation very inefficient. Therefore, organic chromophores, which can absorb UV and/or visible light and transfer energy to Ln^{3+} effectively are employed as light gatherers to stimulate Ln^{3+} emission in a process known as the antenna effect.[12−14] From the hard−soft acid−base theory, multidentate ligands with N- and O-donor atoms are good candidates in the construction of lanthanide complexes. For example, aromatic carboxylic acids[15−19] and β-diketones[20−25] have been investigated extensively in recent decades.

Carprofen, 6-chloro-α-methylcarbazole-2-acetic acid, as shown in Supporting Information Figure S1, is a nonsteroidal anti-inflammatory drug (NSAID) belonging to the class of 2-arylpropionic acid. It has attracted much attention in pharmaceutical and commercial applications. From the viewpoint of pharmacology, carprofen prevents the transformation of arachidonic acid into prostaglandins and thromboxane A2. Therefore, it provides potent treatment for pain and inflammation.[26] From the standpoint of coordination chemistry, the major portion of carprofen molecular structure is a carbazole ring including the delocalized π-electron system which can absorb ultraviolet light and transfer the energy to a central metal ion. Hence, carprofen is expected to have good coordination and effective energy transfer to lanthanide ions. The current interest in metallotherapeutic drugs has motivated the design of anticancer lanthanide compounds.[27,28] The study of lanthanide−carprofen complexes has not been reported; hence, in this article, new Eu and Tb carprofen complexes have been synthesized by a hydrothermal method. The fundamental coordination structure, the basic photophysical properties, and the energy transfer from the carprofen ligand to the central lanthanide ions have been studied. The new compounds might combine the advantages of the nonsteroidal anti-inflammatory drug and the luminescence of the lanthanide ions with the potential application as target medicine.

2. EXPERIMENTAL SECTION

2.1. Materials. Carprofen was kindly donated by Professor Zhongning Yin of Sichuan University. Eu_2O_3 (99.99%), Tb_4O_7 (99.99%), NaOH (AR), ethanol (AR), *N*,*N*-dimethylformamide (AR), and hydrochloric acid (AR) were used as starting materials.

Received: May 29, 2014
Published: November 17, 2014

   dx.doi.org/10.1021/ic501252x | *Inorg. Chem.* 2014, 53, 12275−12282

$LnCl_3$ (Ln = Eu^{3+} and Tb^{3+}) reagents were prepared by dissolution of the corresponding lanthanide oxides (0.5 mmol Eu_2O_3 or 0.25 mmol Tb_4O_7) with concentrated hydrochloric acid, and then repeated evaporations until removal of the excess hydrochloric acid.

2.2. Synthesis of the Samples. Complex **1** was synthesized by a hydrothermal method. A 2.5 mmol portion of NaOH was added to 25 mL of DMF/H_2O (4:1 by volume) solution containing of 3 mmol carprofen with stirring for 20 min. Then 1 mmol $EuCl_3$ aqueous solution was added dropwise to this mixture. A white precipitate formed immediately, and the reaction mixture was stirred vigorously for 3 h at room temperature. Thereafter, the pH of the mixture was adjusted to ~6, and it was transferred to a 50 mL Teflon reactor kept at 160 °C for 80 h under autogenous pressure. Subsequently, the vessel was cooled to room temperature, and the solid was filtered, washed with 10 mL of distilled H_2O, and dried at room temperature. Yellow block single crystals suitable for single-crystal X-ray diffraction experiments were obtained by slow solvent evaporation from the clear filtered solution in several days. Anal. Calc (%) for $C_{96}H_{80}Cl_6Eu_2N_8O_{14}$: C, 55.23; H, 3.84; N, 5.37. Found: C, 54.52; H, 4.10; N, 5.13. FTIR (KBr pellet; cm^{-1}): 3412, 2967, 2929, 1655, 1591, 1529, 1473, 1456, 1409, 1374, 1065, 933, 894, 868, 810, 739, 680.

The synthesis procedure of **2** is similar to that of **1** except that $EuCl_3$ was replaced by $TbCl_3$. Unfortunately, crystals suitable for single-crystal XRD were not obtained. Anal. Calc (%) for $C_{96}H_{80}Cl_6Tb_2N_8O_{14}$: C, 54.86; H, 3.81; N, 5.33. Found: C, 54.70; H, 3.93; N, 4.84. FTIR (KBr pellet; cm^{-1}): 3428, 2967, 2934, 1658, 1542, 1472, 1460, 1420, 1273, 1065, 935, 871, 806, 582.

2.3. Physical Measurements. The FTIR spectra were recorded in the range 4000−400 cm^{-1} by a PerkinElmer spectrum 65 FTIR instrument by the KBr pellet technique. The electronic absorption spectra of the ligand and the complexes in ethanol solution at the concentration of ~10^{-4} M were measured by a Persee TU-1901 UV−Vis spectrophotometer. The photoluminescence (PL) spectra, lifetime measurements, and time-resolved spectra were recorded by an Edinburgh FLS920 fluorescence spectrometer equipped with a 450 W xenon lamp and a pulsed xenon lamp as the excitation sources and a Shimidazu R9287 PMT as the detector. The overall quantum yields ($\Phi_{overall}$'s) were measured by an integrating sphere in the FLS920 fluorescence spectrometer. The powder and the solution samples were placed in the sphere and the Xe lamp was employed as the light source to pump the samples. The $\Phi_{overall}$ was obtained by comparing the spectral intensities of the light source and the sample emission.[29] A Janis Research closed cycle cooling system was used to provide a low temperature environment (to 10 K and below) for the samples.

X-ray Crystallographic Study. A suitable crystal of **1** with dimensions (mm^3) of 0.32 × 0.28 × 0.22 was selected for the single-crystal X-ray diffraction study. The diffraction data were collected at 170 K on an Oxford Xcalibur (Atlas Gemini ultra) diffractometer equipped with a low-temperature device and a graphite-monochromated Mo Kα (λ = 0.710 73 Å) radiation source. The structure was solved by direct methods and refined by the full-matrix least-squares on F^2 using the SHELXTL-97 program. All non-hydrogen atoms were refined with anisotropic displacement parameters. The hydrogen atoms were positioned geometrically (C−H, 0.95 and 1.0 Å; N−H, 0.95 Å).

3. RESULTS AND DISCUSSION

3.1. X-ray Crystal Structures. The solid state structure of $[Eu_2(carprofen)_6(DMF)_2]$ (**1**) was determined by single-crystal X-ray diffraction. Crystal data and structure refinement parameters are listed in Table 1. The complex **1** crystallizes in the monoclinic space group *C2/c*. Figure 1 presents the molecular structure of this complex. As shown in the figure, the molecule consists of a homodinuclear form, in which two europium atoms are bridged by four oxygen atoms from four carprofen ligands in various coordination modes. The bridging binding modes (see Supporting Information Figure S2) that contain two bidentate and two tridentate bridges can be termed as $(\mu:\eta^1-\eta^1)_2(\mu:\eta^2-\eta^1)_2$. Each europium atom is eight-coordinated by seven carboxyl oxygen atoms and one carbonyl oxygen atom of coordinated DMF. It is worth noting that the dimeric structure of complex **1** has an inversion center of symmetry, which suggests that the Eu(1) and Eu(1)a centers reside in the equivalent coordinational environments.[15] The distance between Eu(1) and Eu(1)a centers is 3.8075 Å, which is shorter than that has been reported in other Eu^{3+} carboxylate complexes featuring a homodinuclear structure.[15,16,30−34] The relatively short Eu−Eu distance possibly results from the $(\mu:\eta^1-\eta^1)_2(\mu:\eta^2-\eta^1)_2$ bridging binding mode. The Eu−O bond lengths are in the range 2.315−2.485 Å, which is in agreement with the literature values observed for Eu^{3+} carboxylate complexes.[15,16,30−34] The longest Eu−O bonds involve the oxygen atoms of the bidentate chelating ligands [Eu(1)−O(6), 2.473 Å] and tridentate bridging ligands [Eu(1)−O(1), 2.485 Å; Eu(1)−O(2), 2.473 Å]. The shortest Eu−O bonds are associated with the bidentate bridging ligand [Eu(1)−O(3)a, 2.315 Å; Eu(1)−O(4), 2.346 Å] and the coordinated DMF [Eu(1)−O(7), 2.345 Å].

Table 1. Crystal Data and Structure Refinement Parameters of Complex 1

formula	$C_{96}H_{80}Cl_6Eu_2N_8O_{14}$
fw	2086.30
wavelength (Å)	0.710 73
a (Å)	33.2220(17)
b (Å)	14.2730(4)
c (Å)	22.5073(12)
α (deg)	90
β (deg)	124.968(8)
γ (deg)	90
T (K)	170
V ($Å^3$)	8745.8(7)
space group	*C2/c*
reflns collected	26 780
unique reflns	7999
obsd reflns	6710
R_{int}	0.0377
D_{calcd} (g cm^{-3})	1.584
Z	4
μ(Mo, Kα) (mm^{-1})	1.675
F(000)	4208.0
θ max. (deg)	25.350
R1 ($I > 2\sigma I$)	0.0314
wR2 (all data)	0.0674
GOF	1.048

The selected bond lengths and bond angles are listed in Table 2. The coordination polyhedron around the central Eu^{3+} can be described as a distorted trigonal dodecahedron (see Supporting Information Figure S3(a)) formed by one chelating carboxyl, two bidentate bridging ones, two tridentate bridging ones, and one DMF molecule. At the same time, the geometry of the Eu(1) atom can also be stated as a distorted square antiprism as shown in Supporting Information Figure S3(b), in which the top square face is composed by O(1), O(2), O(3)a, and O(7), while the bottom face is formed by O(2)a, O(4), O(5), and O(6). The dihedral angle between the square faces is 9.16°. The corresponding O−Eu−O bond angles range from 52.25(8)° to 160.04(8)°. Due to the tridentate type, the carboxylate group is rather asymmetric. In fact, the C−O

dx.doi.org/10.1021/ic501252x | *Inorg. Chem.* 2014, 53, 12275−12282

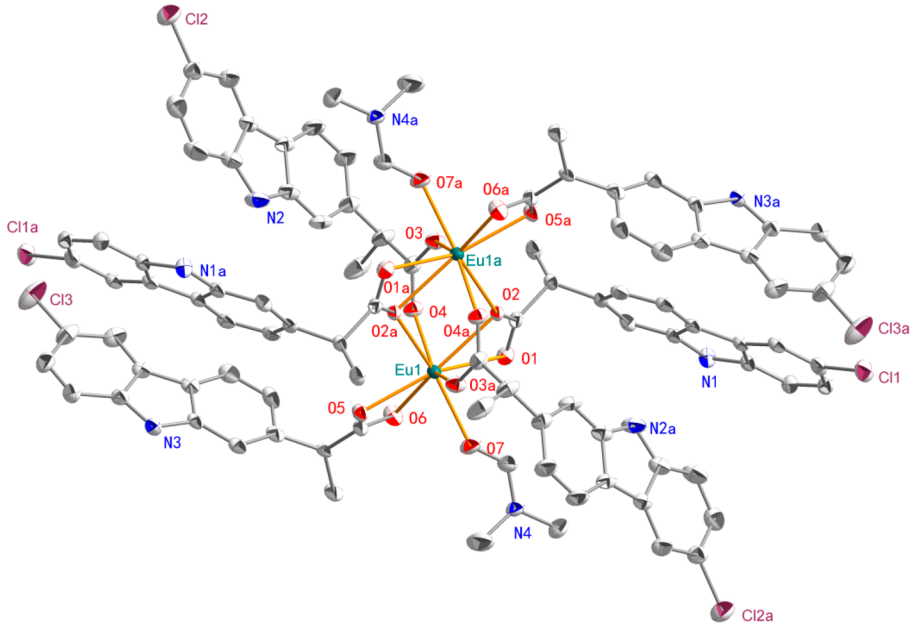

Figure 1. Dimeric structure of complex **1** with thermal ellipsoids at 40% probability. All hydrogen atoms have been omitted for clarity. Symmetry codes: (a) 1.5 − *x*, 1.5 − *y*, 2 − *z*.

Table 2. Selected Bond Lengths (Å) and Bond Angles (deg) for Complex 1[a]

Eu(1)−Eu(1)a	3.8075(3)	Eu(1)−O(2)	2.473(2)	Eu(1)−O(1)	2.485(2)
Eu(1)−O(3)a	2.315(2)	Eu(1)−O(6)	2.473(2)	Eu(1)−O(2)a	2.401(2)
Eu(1)−O(7)	2.345(2)	Eu(1)−O(4)	2.346(2)	Eu(1)−O(5)	2.409(2)
O(3)a−Eu(1)−O(7)	78.01(10)	O(4)−Eu(1)−O(6)	79.72(8)	O(2)a−Eu(1)−O(6)	121.20(8)
O(7)−Eu(1)−O(2)a	149.52(9)	O(3)a−Eu(1)−O(1)	109.85(9)	O(3)a−Eu(1)−O(4)	139.41(8)
O(4)−Eu(1)−O(2)a	71.16(8)	O(7)−Eu(1)−O(1)	77.03(9)	O(7)−Eu(1)−O(4)	139.27(9)
O(3)a−Eu(1)−O(5)	94.84(8)	O(4)−Eu(1)−O(1)	74.57(8)	O(5)−Eu(1)−O(6)	53.30(8)
O(2)a−Eu(1)−O(5)	83.33(7)	O(2)−Eu(1)−O(1)	52.25(8)	O(3)a−Eu(1)−O(2)a	73.90(8)
O(3)a−Eu(1)−O(2)	75.47(8)	O(6)−Eu(1)−O(1)	94.09(8)	O(2)−Eu(1)−O(6)	143.23(8)
O(7)−Eu(1)−O(2)	106.97(9)	O(7)−Eu(1)−O(6)	73.81(9)	O(7)−Eu(1)−O(5)	87.53(9)
O(4)−Eu(1)−O(2)	77.25(8)	O(4)−C(30)−O(3)	124.3(3)	O(2)a−Eu(1)−O(1)	123.71(8)
O(2)a−Eu(1)−O(2)	77.25(8)	O(6)−C(45)−O(5)	120.5(3)	O(4)−Eu(1)−O(5)	100.93(8)
O(5)−Eu(1)−O(2)	160.04(8)	O(1)−C(15)−O(2)	119.8(3)	O(5)−Eu(1)−O(1)	147.00(8)
O(3)a−Eu(1)−O(6)	137.53(8)				

[a]Symmetry codes: (a) 1.5 − *x*, 1.5 − *y*, 2 − *z*; (b) *x*, 1 + *y*, *z*; (c) 1.5 − *x*, −0.5 + *y*, 1.5 − *z*.

distances for the two tridentate bridging carboxylate groups are 1.2492(4) Å (involving the monodentate oxygen atom), 1.2741(4) Å (involving the bidentate oxygen atom), respectively. Meanwhile, the symmetrical bidentate bridging and chelating C−O bond lengths are (1.2630(4) Å, 1.2560(4) Å) and (1.2589(4) Å, 1.2636(4) Å), respectively. The O−C−O angle range for the different carboxylate groups varies from 119.8° to 124.3°, which can be attributed to different coordination modes.

Being considerably strong and highly directional, hydrogen bonding interaction is widely utilized to generate novel supramolecular topological structures. In this work, a wide variety of intramolecular and intermolecular hydrogen bonds have been observed in the structure of complex **1** (Table 3). The packing diagram for complex **1** reveals the presence of a 1D molecular array (along the *b* axis) that is illustrated by the intermolecular hydrogen bonds between N(3) and O(5) through H(3) with a H···O distance of 2.1682 Å and a N−H···O angle of 147.546° (Figure 2). The chains are connected along the *c* axis by the intermolecular hydrogen bonding interaction between N(1)c and O(6) through H(1)c with a H···O distance of 2.1187 Å and a C−H···O angle of 152.243°,

Table 3. Distances (Å) and Angles (deg) of Hydrogen Bonds[a]

D−H···A	*d*(D−H)	*d*(H···A)	*d*(D···A)	∠(DHA)
N(3)−H(3)···O(5)a	0.8800(25)	2.1682(23)	2.9481(34)	147.546(209)
N(1)c−H(1)c···O(6)	0.8805(28)	2.1187(30)	2.9267(43)	152.243(193)
C(1)c−H(1)c···O(1)	0.9498(41)	2.7821(21)	3.4230(34)	125.574(220)
C(1)c−H(1)c···O(4)	0.9498(41)	2.7411(29)	3.6671(51)	165.098(219)
C(31)b−H(31)b···O(5)	0.9489(36)	2.7417(23)	3.4153(43)	128.611(271)
C(13)−H(13)···O(5)a	0.9989(54)	2.4481(30)	3.3726(58)	153.655(237)
C(10)−H(10)···O(5)a	0.9498(50)	2.7393(34)	3.5595(64)	145.044(259)

[a]Symmetry codes: (a) 1.5 − *x*, 1.5 − *y*, 2 − *z*; (b) *x*, 1 + *y*, *z*; (c) 1.5 − *x*, −0.5 + *y*, 1.5 − *z*.

dx.doi.org/10.1021/ic501252x | *Inorg. Chem.* 2014, 53, 12275−12282

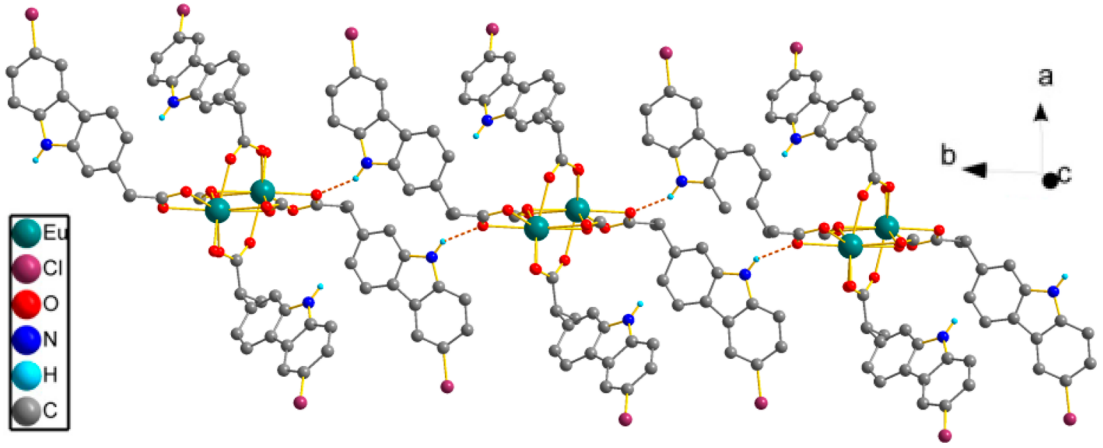

Figure 2. 1D linear structure of complex **1** connected via N−H···O hydrogen bonds (along the *b* axis). All C−H hydrogen atoms, the coordinated DMF molecules, and a third of coordinated carprofen molecules have been omitted for clarity.

generating a 2D network extending along the *bc* plane (Supporting Information Figure S4). The 2D framework is further assembled by N−H···O and C−H···O hydrogen bonding to form a 3D supramolecular framework.

3.2. FTIR Results and Analysis. The infrared spectra of the complexes and the ligand are displayed in Supporting Information Figure S5. The free carprofen ligand exhibits an intense C═O stretching vibration band at 1698 cm^{-1}. In the FTIR spectrum of complexes **1** and **2**, the ν(O−H) in the range 2600−3300 cm^{-1} and ν(C═O) of carboxyl group at 1698 cm^{-1} disappear, which confirms the coordination of the carprofen ligand to the corresponding Ln^{3+}. In **1**, the $\nu_{as}(COO^-)$ and $\nu_s(COO^-)$ bands split into two peaks at (1591 cm^{-1}, 1529 cm^{-1}) and (1409 cm^{-1}, 1374 cm^{-1}), respectively. The difference between the asymmetric and symmetric stretching vibration ($\Delta\nu(COO^-) = \nu_{as} - \nu_s$) is 217 and 120 cm^{-1}, indicating the coordination of Eu^{3+} ions with carprofen groups is chelating and bridging modes,[15,35] which is in agreement with the XRD analysis results. In addition, the FTIR spectra of complex **1** and **2** display an apparent band at 1655 and 1658 cm^{-1}, respectively, which is attributed to the ν(C═O) of coordinated DMF, and it presents a bathochromic shift as compared with that in free DMF [ν(C═O) is 1670 cm^{-1}].[36]

3.3. UV−Vis Spectra. The UV−Vis absorption spectra of the free carprofen ligand and the corresponding complexes **1** and **2** were measured in ethanol solution at the concentration of ~10^{-4} M and are displayed in Supporting Information Figure S6. The absorption bands at 239, 263, and 301 nm for the ligand can be assigned to the singlet−singlet π−π* absorptions of the carbazole ring, while the absorption bands at 331 and 345 nm arise probably from the n−π* transition of the free ligand.[37] No significant change is observed in the position and the shape of the absorption of the lanthanide complexes; therefore, it illustrates that the coordination of the Ln^{3+} ion does not change the energy of the singlet state of the carprofen ligand dramatically.

3.4. Photophysical Properties of the Complexes. The excitation and emission spectra of the free ligand (Supporting Information Figure S7) and the complexes **1**−**2** (Figures 3 and 4) in the solid state have been studied at room temperature. As compared with the excitation spectrum profiles of the pure ligand and the complexes, one can see that, in **1**, the Eu^{3+} characteristic f−f transition peaks dominate and the absorption

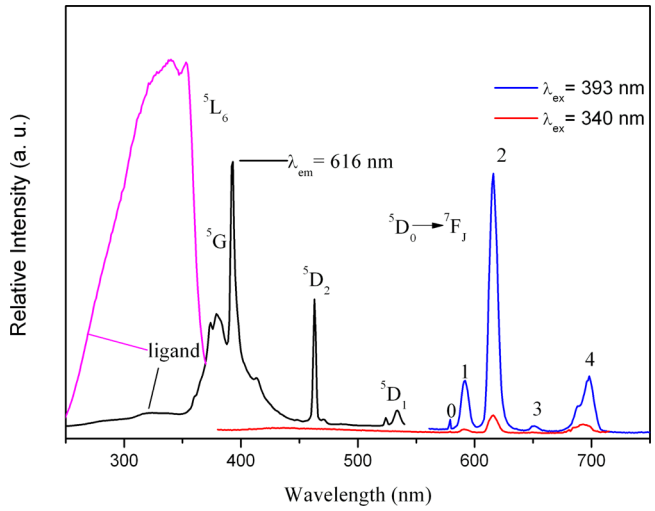

Figure 3. PL and PLE spectra of **1** in solid state at room temperature. The excitation spectrum of the carprofen ligand (magenta curve) is also included in the figure.

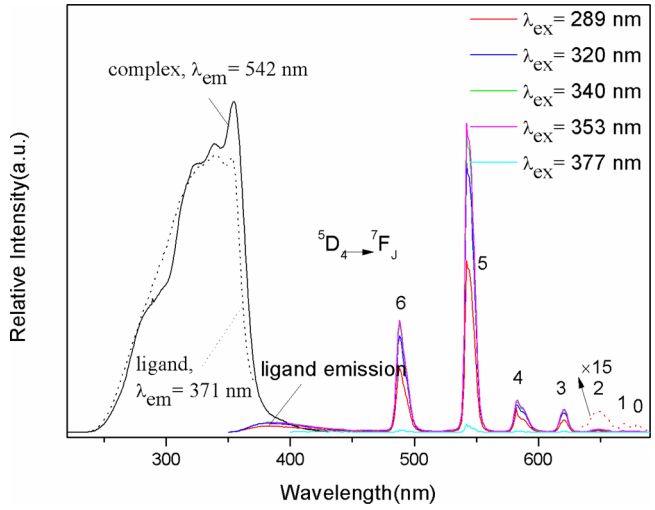

Figure 4. PL and PLE spectra of **2** in solid state at room temperature. The excitation spectrum of the carprofen ligand (black dot curve) is also included. The dotted curve on the right-hand side is the magnification of $^5D_4$ to ^7F_J (J = 2, 1, 0) transitions.

dx.doi.org/10.1021/ic501252x | *Inorg. Chem.* 2014, 53, 12275−12282

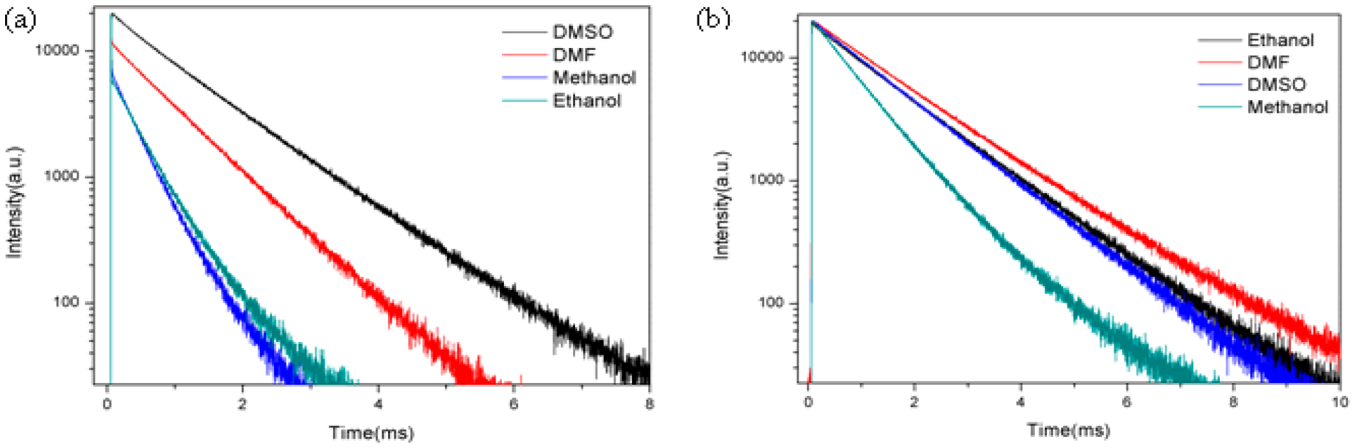

Figure 5. Luminescence decay curves of **1** (a) and **2** (b).

Table 4. Luminescent Decay Data and the Quantum Yields of Complexes 1 and 2

	Eu $^5D_0$				Tb $^5D_4$			
medium	τ_1 (μs) (B_1)[a]	τ_2 (μs) (B_2)[a]	$\langle\tau\rangle$ (μs)	$\Phi_{overall}$[b]	τ_1 (μs) (B_1)[a]	τ_2 (μs) (B_2)[a]	$\langle\tau\rangle$ (μs)	$\Phi_{overall}$[b]
solid	139 (32%)	470 (68%)	362	0.11%	757 (25%)	1358 (75%)	1210	9%
MeOH	324 (75%)	705 (25%)	421	<0.1%	758 (86%)	1645 (14%)	880	4%
EtOH	401 (83%)	1036 (17%)	510	<0.1%	888 (11%)	1422 (89%)	1362	3%
DMF	842			<0.1%	1470			2%
DMSO	1117			<0.1%	1281			5%

[a] B_1 and B_2 are the percentages of short- and long-decay components. [b] The overall quantum yields of the complexes recorded by the integrating sphere. The emission of **1** was very weak, and the quantum yields are tentative.

band of the ligand (and the charge transfer band of Eu^{3+}–O^{2-}) is very weak. At the same time, from the emission spectrum of **1**, it is found that the direct excitation (λ_{ex} = 393 nm) is much more efficient than that of the indirect excitation (λ_{ex} = 340 nm). However, for **2**, when the green emission of Tb^{3+} is monitored, the excitation spectrum is almost identical with that of the pure ligand. The f–f and the f–d transitions of Tb^{3+} are not obviously observed. This shows that the carprofen ligand is a better sensitizer for Tb^{3+} ions than for Eu^{3+} ions in this study.

The overall quantum yields and the sensitization efficiency of the ligand were also investigated. The sensitization efficiency is calculated from the following equation:[1]

$$\Phi_{sen} = \Phi_{overall}/\Phi_{Ln} \quad (1)$$

Here $\Phi_{overall}$ is the overall luminescence quantum yield for a lanthanide complex; Φ_{sen} represents the sensitization efficiency, which illustrates the energy transfer efficiency between the ligand and the central lanthanide ions; and Φ_{Ln} stands for the intrinsic quantum yield of Ln^{3+} ion. The $\Phi_{overall}$ values of **1** and **2** in the solid state were recorded to be 0.11% and 9%, respectively. Φ_{Tb} was obtained from the direct excitation experiments, and Φ_{Eu} was calculated by eqs 2 and 3.[38]

$$\Phi_{Eu} = \left(\frac{A_{RAD}}{A_{RAD} + A_{NR}}\right) = \frac{\tau_{obs}}{\tau_{RAD}} \quad (2)$$

$$A_{RAD} = \frac{1}{\tau_{RAD}} = A_{MD,0} n^3 \left(\frac{I_{TOT}}{I_{MD}}\right) \quad (3)$$

The detailed information about the parameters and the values used to calculate Φ_{Eu} are documented in ref 38. $\Phi_{sen,Tb}$ is calculated to be 75%, and $\Phi_{sen,Eu}$ is calculated to be 1%. The obtained sensitization efficiency of **2** is much higher than that of **1**, which is consistent with the results of fluorescence spectra. The reason why these two complexes show greatly different sensitization efficiencies will be discussed in the later section.

To study the effect of solvents on the luminescence of the complexes, the emission spectra and the lifetimes of complexes **1** and **2** were measured both in the solid state and in different solvents at room temperature. The corresponding emission spectra in the solvents can be found in Supporting Information Figures S8 and S9. From these figures, one can see that actually the emission spectra of these compounds in solvents show different emission intensities, which might be caused by the dissociation of the compounds and/or the different vibronic oscillator effect. The decay profiles are depicted in Figure 5. The detailed lifetimes are exhibited in Table 4. The relatively shorter lifetime observed for **1** in the solid state and solution may be attributed to the radiationless transition process that is associated with vibronic coupling due to the presence of solvent molecules. The $^5D_0$ (Eu^{3+}) and $^5D_4$ (Tb^{3+}) lifetimes were obtained from the luminescent decay profiles for complexes **1** and **2** at room temperature. It was found that the luminescence decay profiles obeyed a double exponential expression

$$I(t) = A + B_1 \exp(-t/\tau_1) + B_2 \exp(-t/\tau_2) \quad (4)$$

where τ_1 and τ_2 are short- and long-decay components, respectively. The lifetime values (μs) of Tb^{3+} complex in the solid state are determined to be 757 and 1358, and 139 and 470 for the Eu^{3+} complex, respectively. The mean lifetimes $\langle\tau\rangle$ are 1210 μs for Tb^{3+} and 362 μs for Eu^{3+} calculated by the equation[39]

$$\langle\tau\rangle = (B_1\tau_1^2 + B_2\tau_2^2)/(B_1\tau_1 + B_2\tau_2) \quad (5)$$

where B_1 and B_2 are weight factors.

dx.doi.org/10.1021/ic501252x | Inorg. Chem. 2014, 53, 12275–12282

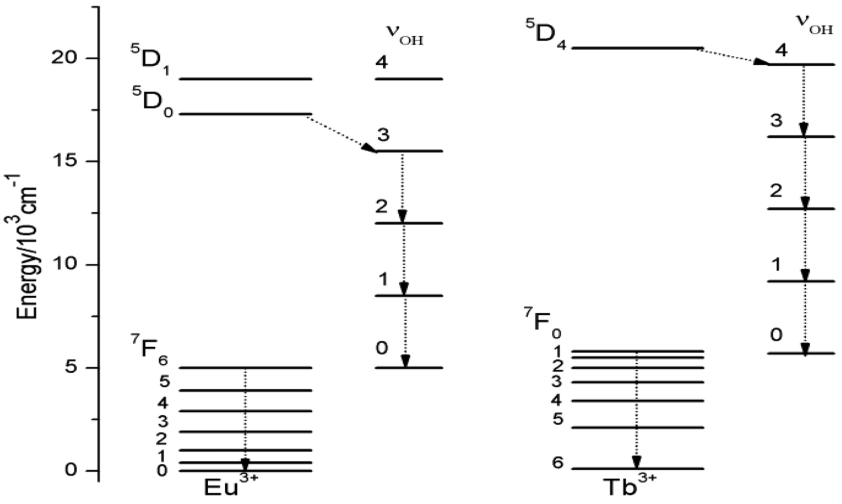

Figure 6. Deactivation of the luminescence from $^5D_0$ and $^5D_4$ in solution occurs by means of a vibrational energy transfer process involving O−H.

The effect of solvent molecules on the luminescent lifetime of Eu and Tb complexes was investigated using MeOH, EtOH, DMF, and DMSO. Complexes **1** and **2** are soluble in all these solvents. The lifetimes in DMSO and DMF are obviously larger than those in MeOH and EtOH, as shown in Table 4. The lifetime values increased in the order of MeOH (421 μs) < EtOH (510 μs) < DMF (842 μs) < DMSO (1117 μs), which suggests that the shorter lifetimes in the hydroxyl-containing solvents should be due to the vibration of O−H relaxation processes for the Eu^{3+} ion. On the other hand, the lifetime values of $^5D_4 \rightarrow {}^7F_5$ (Tb^{3+}) increased in the order of MeOH (880 μs) < DMSO (1281 μs) < EtOH (1362 μs) < DMF (1470 μs). The nonradiative relaxation via vibronic coupling has been considered as a primary process that quenches the excited states of $^5D_0$ for Eu^{3+} and $^5D_4$ for Tb^{3+} in liquid systems.[39−41] The excited states of $^5D_0$ (Eu^{3+}) and $^5D_4$ (Tb^{3+}) are usually relatively long (microseconds to milliseconds time scale),[9,11] which enable energy transfer to high frequency vibrational oscillators such as O−H, N−H, and C−H. As a consequence, the presence of these groups in the proximity of the central ion favors quenching of the luminescence.[40−43] In particular, the smaller the energy gap between the excited state and the next level below it, then the more efficient the deactivation by vibronic coupling will be.[44] It is known that the vibronic coupling probability is proportional to the Franck−Condon factor F,[40,43] which could be estimated quantitatively as a function of the vibrational quantum number ν and vibration energy γ when the approximation of the undistorted oscillator model is adopted. F decreases with increasing ν if γ is assumed to be constant.[43] The energy levels of the multiplets of Eu^{3+} and Tb^{3+} are known, and the possible deactivation of the $^5D_0$ (Eu^{3+}) and $^5D_4$(Tb^{3+}) in solutions occurs by means of a vibrational energy transfer process involving OH as schematically illustrated in Figure 6. One can see from the figure that the energy gap between the crucial radiative and ground state manifolds of Eu^{3+} (the energy difference between $^5D_0$ and $^7F_6$) is approximately 12 300 cm^{-1}, matching well the vibrations of O−H bonds ($\nu_{OH} \approx$ 3300−3500 cm^{-1}) with vibrational quantum number ν = 3, which leads to effective quenching of the excited state of Eu^{3+}. Meanwhile, in the Tb^{3+} system, the energy gap is about 14 800 cm^{-1} ($^5D_4 \rightarrow {}^7F_0$), and the matching occurs with vibrational quantum number ν = 4. Here, the vibrational quantum number in the Tb^{3+} complex is bigger than that in the Eu^{3+} complex, which leads to smaller Franck−Condon factor F and the smaller vibronic coupling probability. It is consistent with the less efficient quenching observed in the case of Tb^{3+} in hydroxyl-containing solvent on account of the minor Franck−Condon overlap factor.

3.5. Intramolecular Energy Transfer in 1 and 2. In order to understand the energy transfer processes, the singlet and triplet energy levels of the ligand were determined. In our study, the time-resolved emission spectroscopy (TRES) of the ligand is recorded at 10 K to determine the energy of the triplet state of the ligand, which is displayed in Figure 7. Upon enforcing an 8 ns delay time, fluorescence of the ligand almost disappears, while weak phosphorescence is detected with a maximum at 391 nm. The triplet ($^3\pi\pi^*$) energy level of the ligand can be estimated to be approximately 384 nm (26 042 cm^{-1}) by reference to the lower wavelength emission edge from the low-temperature time-resolved phosphorescence spectra.[45] The singlet ($^1\pi\pi^*$) energy level lies at about 309 nm (32 362 cm^{-1}), as estimated from the higher wavelength edge of the UV−vis absorption of the ligand.[46,47] According to Reinhoudt's empirical rule,[48] the intersystem crossing process becomes effective when ΔE ($^1\pi\pi^*-{}^3\pi\pi^*$) is at least 5000 cm^{-1}. The

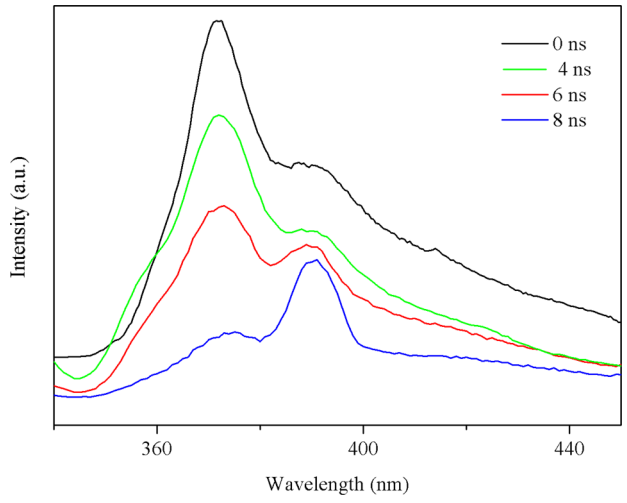

Figure 7. Time-resolved emission spectroscopy (TRES) of the ligand excited at 280 nm at 10 K.

dx.doi.org/10.1021/ic501252x | *Inorg. Chem.* 2014, 53, 12275−12282

energy gap ΔE ($^1\pi\pi^*-^3\pi\pi^*$) for carprofen ligand in this study is 6360 cm^{-1}. As a consequence, the intersystem crossing process is effective for this ligand. From Latva's empirical rule,[49] the energy difference between the triplet state $^3\pi\pi^*$ of the ligand and the ^5D_J levels of Tb^{3+} or Eu^{3+} is in the range 2000–5000 cm^{-1}, which favors the optimal ligand-to-metal energy transfer process.

The energy gap ΔE ($^3\pi\pi^*-^5D_4$) for Tb^{3+} is 5497 cm^{-1} in this study, suggesting that the carprofen ligand can serve as a relatively effective antenna for Tb^{3+}. However, the energy gap ΔE ($^3\pi\pi^*-^5D_0$) for Eu^{3+} is 8759 cm^{-1}, being too large to be an effective energy transfer. Therefore, the carprofen ligand matches better the emissive $^5D_4$ state of Tb^{3+} at 20 545 cm^{-1} and hence leads to a more efficient sensitization of the terbium complex than that in the europium complex.

4. CONCLUSIONS

Two new lanthanide complexes $[Eu_2(carprofen)_6(DMF)_2]$ and $[Tb_2(carprofen)_6(DMF)_2]$ have been successfully synthesized by a hydrothermal method. The structure of the Eu complex has been determined by single-crystal X-ray diffraction. The complexes exhibit appropriately efficient photoluminescence upon irradiation with UV light, suggesting energy transfer from the antenna ligand to Ln^{3+}. However, carprofen is considered to be more suitable for the sensitization of Tb^{3+} than Eu^{3+}, by the investigation of sensitization efficiency as well as the matching of the triplet state of the carprofen ligand with that of emitting levels of the lanthanide ions. The sensitization efficiency of $[Tb_2(carprofen)_6(DMF)_2]$ is calculated to be 75% while that of $[Eu_2(carprofen)_6(DMF)_2]$ is 1%. The poor sensitization of Eu^{3+} complex is probably caused by the larger energy gap between the triplet state of the ligand and the $^5D_0$ level of Eu^{3+}.

■ ASSOCIATED CONTENT

Supporting Information

Structural formula of carprofen, different types of binding modes for the ligand observed in Eu complex, two possible coordination polyhedrons of Eu^{3+} ions, the 2D supramolecular framework formed by hydrogen bonds, the FTIR spectra of the complexes and the ligand, UV–vis absorption spectra of the free ligand and complexes in ethanol solution, room temperature solid state excitation and emission spectra of the free carprofen ligand, and emission spectra of the two complexes in different solvents. Crystallographic data in CIF format. This material is available free of charge via the Internet at http://pubs.acs.org.

■ AUTHOR INFORMATION

Corresponding Author

*E-mail: zhouxj@cqupt.edu.cn. Phone: +86 +23 62471347. Fax: +86 +23 62471347.

Notes

The authors declare no competing financial interest.

■ ACKNOWLEDGMENTS

The project was funded by National Natural Science Foundation of China (10704090, 81373338), Key Project of Chinese Ministry of Education (211154), and Natural Science Foundation Project of Chongqing (KJ110532, CSTC 2012JJA90019, and CSTC2011jjA50016).

■ REFERENCES

(1) Bünzli, J.-C. G.; Piguet, C. *Chem. Soc. Rev.* **2005**, *34*, 1048–1077.
(2) Kuriki, K.; Koike, Y.; Okamoto, Y. *Chem. Rev.* **2002**, *102*, 2347–2356.
(3) Jüstel, T.; Nikol, H.; Ronda, C. *Angew. Chem., Int. Ed.* **1998**, *37*, 3084–3103.
(4) Liu, Y.; Pan, M.; Yang, Q. Y.; Fu, L.; Li, K.; Wei, S. C.; Su, C. Y. *Chem. Mater.* **2012**, *24*, 1954–1960.
(5) de Bettencourt-Dias, A. *Dalton Trans.* **2007**, 2229–2241.
(6) Weibel, N.; Charbonnière, L. J.; Guardigli, M.; Roda, A.; Ziessel, R. *J. Am. Chem. Soc.* **2004**, *126*, 4888–4896.
(7) Picot, A.; D'Aléo, A.; Baldeck, P. L.; Grichine, A.; Duperray, A.; Andraud, C.; Maury, O. *J. Am. Chem. Soc.* **2008**, *130*, 1532–1533.
(8) Petoud, S.; Cohen, S. M.; Bünzli, J.-C. G.; Raymond, K. N. *J. Am. Chem. Soc.* **2003**, *125*, 13324–13325.
(9) Bünzli, J.-C. G. *Chem. Rev.* **2010**, *110*, 2729–2755.
(10) Pandya, S.; Yu, J. H.; Parker, D. *Dalton Trans.* **2006**, 2757–2766.
(11) Moore, E. G.; Samuel, A. P. S.; Raymond, K. N. *Acc. Chem. Res.* **2009**, *42*, 542–552.
(12) Cui, Y. J.; Yue, Y. F.; Qian, G. D.; Chen, B. L. *Chem. Rev.* **2012**, *112*, 1126–1162.
(13) Chen, F. F.; Chen, Z. Q.; Bian, Z. Q.; Huang, C. H. *Coord. Chem. Rev.* **2010**, *254*, 991–1010.
(14) Armelao, L.; Quici, S.; Barigelletti, F.; Accorsi, G.; Bottaro, G.; Cavazzini, M.; Tondello, E. *Coord. Chem. Rev.* **2010**, *254*, 487–505.
(15) Ramya, A. R.; Reddy, M. L. P.; Cowley, A. H.; Vasudevan, K. V. *Inorg. Chem.* **2010**, *49*, 2407–2415.
(16) de Bettencourt-Dias, A.; Viswanathan, S. *Dalton Trans.* **2006**, 4093–4103.
(17) Chen, R. L.; Chen, X. Y.; Zheng, S. R.; Fan, J.; Zhang, W. G. *Cryst. Growth Des.* **2013**, *13*, 4428–4434.
(18) Huang, W.; Wu, D. Y.; Zhou, P.; Yan, W. B.; Guo, D.; Duan, C. Y.; Meng, Q. J. *Cryst. Growth Des.* **2009**, *9*, 1361–1369.
(19) Fang, S. M.; Sañudo, E. C.; Hu, M.; Zhang, Q.; Ma, S. T.; Jia, L. R.; Wang, C.; Tang, J. Y.; Du, M.; Liu, C. S. *Cryst. Growth Des.* **2011**, *11*, 811–819.
(20) Biju, S.; Raj, D. B. A.; Reddy, M. L. P.; Kariuki, B. M. *Inorg. Chem.* **2006**, *45*, 10651–10660.
(21) Li, Y. J.; Yan, B. *Inorg. Chem.* **2009**, *48*, 8276–8285.
(22) Pointillart, F.; Maury, O.; Gal, Y. L.; Golhen, S.; Cador, O.; Ouahab, L. *Inorg. Chem.* **2009**, *48*, 7421–7429.
(23) Raj, D. B. A.; Francis, B.; Reddy, M. L. P.; Butorac, R. R.; Lynch, V. M.; Cowley, A. H. *Inorg. Chem.* **2010**, *49*, 9055–9063.
(24) Biju, S.; Gopakumar, N.; Bünzli, J.-C. G.; Scopelliti, R.; Kim, H. K.; Reddy, M. L. P. *Inorg. Chem.* **2013**, *52*, 8750–8758.
(25) Pereira, C. C. L.; Dias, S.; Coutinho, I.; Leal, J. P.; Branco, L. C.; Laia, C. A. T. *Inorg. Chem.* **2013**, *52*, 3755–3764.
(26) Gálico, D. A.; Holanda, B. B. C.; Guerra, R. B.; Legendre, A. O.; Rinaldo, D.; Treu-Filho, O.; Bannach, G. *Thermochim. Acta* **2014**, *575*, 226–232.
(27) Kwong, W. L. *Anti-Cancer Ytterbium Porphyrin and Iron Polypyridyl Complexes: Synthesis, Cytotoxicity and Bioinformatics Studies.* Ph.D. Thesis, The University of Hong Kong, September 2012.
(28) Kostova, I. *Curr. Med. Chem. Anticancer Agents* **2005**, *5*, 591–602.
(29) Biju, S.; Reddy, M. L. P.; Cowley, A. H.; Vasudevan, K. V. *J. Mater. Chem.* **2009**, *19*, 5179–5187.
(30) Viswanathan, S.; de Bettencourt-Dias, A. *Inorg. Chem.* **2006**, *45*, 10138–10146.
(31) Yu, W. J.; Chen, X.; Li, J.; Li, B.; Zhang, T. L.; Tao, J. *CrystEngComm* **2013**, *15*, 7732–7739.
(32) Bußkamp, H.; Deacon, G. B.; Hilder, M.; Junk, P. C.; Kynast, U. H.; Lee, W. W.; Turner, D. R. *CrystEngComm* **2007**, *9*, 394–411.
(33) Tsaryuk, V.; Kudryashova, V.; Gawryszewskab, P.; Szostak, R.; Vologzhanina, A.; Zhuravlev, K.; Klemenkova, Z.; Legendziewicz, J.; Zolin, V. *J. Photochem. Photobiol., A* **2012**, *239*, 37–46.

(34) Tsaryuk, V. I.; Zhuravlev, K. P.; Vologzhanina, A. V.; Kudryashova, V. A.; Zolin, V. F. *J. Photochem. Photobiol., A* **2010**, *211*, 7−19.
(35) Teotonio, E. E. S.; Brito, H. F.; Felinto, M. C. F. C.; Thompson, L. C.; Young, V. G.; Malta, O. L. *J. Mol. Struct.* **2005**, *751*, 85−94.
(36) Zhou, X. J.; Zhou, K. N.; Wang, Z. L.; Yang, S. G. *Z. Anorg. Allg. Chem.* **2013**, *639*, 121−124.
(37) Xu, H. B.; Li, J.; Shi, L. X.; Chen, Z. N. *Dalton Trans.* **2011**, *40*, 5549−5556.
(38) Bourdolle, A.; Allali, M.; Mulatier, J.-C.; Guennic, B. L.; Zwier, J. M.; Baldeck, P. L.; Bünzli, J.-C. G.; Andraud, C.; Lamarque, L.; Maury, O. *Inorg. Chem.* **2011**, *50*, 4987−4999.
(39) Buddhudu, S.; Morita, M.; Murakami, S.; Rau, D. *J. Lumin.* **1999**, *83*−*84*, 199−203.
(40) Døssing, A. *Eur. J. Inorg. Chem.* **2005**, 1425−1434.
(41) Choppin, G. R.; Peterman, D. R. *Coord. Chem. Rev.* **1998**, *174*, 283−299.
(42) Lis, S. *J. Alloys Compd.* **2002**, *341*, 45−50.
(43) Hasegawa, Y.; Wada, Y.; Yanagida, S. *J. Photochem. Photobiol., C* **2004**, *5*, 183−202.
(44) Tanner, P. A.; Duan, C. K. *Coord. Chem. Rev.* **2010**, *254*, 3026−3029.
(45) Deiters, E.; Eliseeva, S. V.; Bünzli, J.-C. G. *Front. Chem.* **2013**, *1*, http://journal.frontiersin.org/Journal/10.3389/fchem.2013.00015/.
(46) Remya, P. N.; Biju, S.; Reddy, M. L. P.; Cowley, A. H.; Findlater, M. *Inorg. Chem.* **2008**, *47*, 7396−7404.
(47) Shi, M.; Li, F. Y.; Yi, T.; Zhang, D. Q.; Hu, H. M.; Huang, C. H. *Inorg. Chem.* **2005**, *44*, 8929−8936.
(48) Steemers, F. J.; Verboom, W.; Reinhoudt, D. N.; van der Tol, E. B.; Verhoeven, J. W. *J. Am. Chem. Soc.* **1995**, *117*, 9408−9414.
(49) Latva, M.; Takalo, H.; Mukkala, V.-M.; Matachescu, C.; Rodriguez-Ubis, J. C.; Kankare, J. *J. Lumin.* **1997**, *75*, 149−169.